



ARTICLE

## Expansive Soil Stabilization by Bagasse Ash in Partial Replacement of Cement

Waleed Awadalseed<sup>1</sup>, Honghua Zhao<sup>1</sup>, Hemei Sun<sup>2</sup>, Ming Huang<sup>3</sup> and Cong Liu<sup>4,\*</sup>

<sup>1</sup>State Key Laboratory of Structural Analysis for Industrial Equipment, Department of Engineering Mechanics, Dalian University of Technology, Dalian, 116023, China

<sup>2</sup>State Key Laboratory of Structural Analysis for Industrial Equipment, Department of Engineering Mechanics, International Research Center for Computational Mechanics, Dalian University of Technology, Dalian, 116023, China

<sup>3</sup>Department of Geotechnical Engineering, College of Civil Engineering, Hunan University, Changsha, 410082, China

<sup>4</sup>College of Civil Engineering, Fuzhou University, Fuzhou, 350116, China

\*Corresponding Author: Cong Liu. Email: lccong@mail.dlut.edu.cn

Received: 22 June 2022 Accepted: 25 August 2022

### ABSTRACT

This study examined the effects of using bagasse ash in replacement of ordinary Portland cement (OPC) in the treatment of expansive soils. The study concentrated on the compaction characteristics, volume change, compressive strength, splitting tensile strength, microstructure, California bearing ratio (CBR) value, and shear wave velocity of expansive soils treated with cement. Different bagasse ash replacement ratios were used to create soil samples. At varying curing times of 7, 14, and 28 days, standard compaction tests, unconfined compressive strength tests, CBR tests, Brazilian split tensile testing, and bender element (BE) tests were carried out. According to X-ray diffraction (XRD) investigations, quartz and cristobalite make up the majority of the minerals in bagasse ash. Bagasse ash contains a variety of grain sizes, including numerous fiber-shaped particles, according to a scanning electronic microscope (SEM) test. For all of the treated specimens with various replacement ratios, the overall additive content has not changed. The results of the Brazilian split tensile tests demonstrate improved tensile strength for all specimens with various replacement proportions. A lower maximum dry density and a greater optimal water content would result from the substitution of bagasse ash. When the replacement ratio is not more than 20%, the CBR values of the parts replaced specimens are even higher than the cement treatments. The results of BE testing on the treated soils show that there is significant stiffness anisotropy but that it steadily diminishes with curing time and replacement ratio. According to the study, bagasse ash is a useful mineral additive, and the best replacement ratio (CBA20) is 20%.

### KEYWORDS

Expansive soil; bagasse ash; cement; calcium silicate hydrate (CSH); stiffness anisotropy

### Nomenclature

$SiO_2$	silica
$Al_2O_3$	Aluminum oxide
$Ca(OH)_2$	Calcium hydroxide
$CO_2$	Carbon dioxide
$SiO_2$	Silicon dioxide



This work is licensed under a Creative Commons Attribution 4.0 International License, which permits unrestricted use, distribution, and reproduction in any medium, provided the original work is properly cited.

$CaO$	Calcium oxide
$MgO$	Magnesium oxide
$Fe_2O_3$	Ferric oxide
$TiO_2$	Titanium dioxide
$K_2O$	Potassium oxide
$ZnO$	Zinc oxide
$Ca^{2+}$	Calcium ion
$T$	tensile strength
$p$	maximum applied load
$l$	length
$d$	diameter
$G_0$	initial shear modulus
$\rho$	mass density of soil
$v$	shear wave velocity
$i$	direction of shear wave propagation
$j$	direction of vibration of soil particles
$v_s$	shear wave in vertical direction
$h$	direction of vibration of soil particles
$G$	shear-modulus
$G_{ivh}/G_{ihh}, G_{ivh}/G_{ihv}, G_{ihh}/G_{ihv}$	stiffness anisotropy ratio
CBA0	Cement: bagasse ash ratio 100:0
CBA10	Cement: bagasse ash ratio 90:10
CBA20	Cement: bagasse ash ratio 80:20
CBA30	Cement: bagasse ash ratio 70:30
CBA40	Cement: bagasse ash ratio 60:40
CBA60	Cement: bagasse ash ratio 40:60
CBA70	Cement: bagasse ash ratio 30:70

## 1 Introduction

Geotechnical engineers have long been concerned with expansive soil treatment, and many different methods and materials have been used [1,2]. When exposed to moisture fluctuations, expansive soil shows considerable volume change. Montmorillonite, illite, and kaolinite are the most common clay minerals found in it. Due to the strong hydrophilicity of these cohesive minerals, expansive soil has swelling and shrinking characteristics in wet and dry conditions. The shrinking and swelling characteristics of expansive soil cause the deformation of buildings, such as displacement, cracking, and slanting. As a result, this sort of soil can result in significant economic losses for countries that have expansive soils in their territories [3]. Soil stabilization, which is separated into two types: mechanical stabilization and chemical stabilization, is an effective approach to remediating expansive soil. This research emphasizes chemical stabilization, which is defined as the process of adding compounds to expansive soil in order to change its properties in order to suit engineering needs. Cement is one of the most essential materials used in soil treatment since it affects the soil's compressive strength, bearing capacity, and compressibility for a variety of purposes. With increasing cure time, cement-treated soil generally becomes more resistant [4,5]. The use of cement in soil treatment has some environmental and financial drawbacks. A substantial volume of carbon dioxide is created during the cement-making process. As a result, partial replacements for cement must be developed in order to reduce cement usage [6].

Pozzolan material is one of the most viable solutions for partial cement replacement because of its low cost and environmental friendliness. Pozzolan material is made up of silicon dioxide ( $SiO_2$ ) and aluminum oxide ( $Al_2O_3$ ). These chemicals react with calcium hydroxide ( $Ca(OH)_2$ ), a byproduct of the cement hydration process to generate new cement components. Various pozzolan materials, such as sludge and bottom ash, are industrial and agricultural wastes that have been employed in soil stabilization around the world [7–9]. Bagasse ash has been one of the materials that has grown more widely employed as a soil stabilizer in recent years due to its renewable nature and lower cost. Bagasse ash is a byproduct of the sugar manufacturing process that is created by burning bagasse fiber. Around 1.5 billion tonnes of sugar cane are produced each year, with 40% to 45% of the residue remaining. Bagasse ash includes a high amount of silica, making it an excellent additive for increasing the characteristics of soil, concrete, and other construction materials when combined with cement or lime [10]. Bagasse is also one of the biomass sources that is frequently employed as a primary energy source. Burning bagasse as an energy source produces ash, which is considered a waste that causes environmental concerns [11]. Bagasse is produced in a number of countries across the world, particularly in areas with a tropical environment. Bagasse production is estimated to be more than 600 million tonnes per year worldwide [12]. It is regarded as an alternative energy source since it has a high amount of silica [13]. The vast volume of bagasse ash from different sources takes up a lot of space and has become a major environmental issue. Several academics have expressed an interest in the potential application of bagasse ash in construction technologies. Li et al. [14,15] provided a summary of the usage study of bagasse ash in concrete between 2000 and 2021, as well as an investigation into the impact of bagasse ash on the microstructure characteristics of concrete, in addition to a physical and chemical analysis of high-volume fly ash. Furthermore, the potential benefits of using bagasse ash in the production of Portland cement, both economically and environmentally, were examined. Li et al. also provided a needs assessment analysis for potential future studies on the utilization of bagasse ash [14,15]. Additionally, the utilization of bagasse ash has expanded to include a variety of different applications, including making silica gel as an adsorbent and catalyst [16].

The use of bagasse ash in the field of soil stabilization has been extensively researched in recent years. Looking through the literature, various analysis methods have been used to examine the utilization of bagasse ash as a partial cement replacement additive. However, these various studies address specific geotechnical issues, but some other aspects did not get enough attention, such as the small strain stiffness of bagasse ash and cement-expansive soil mixtures. The key highlight of this research is, however, providing a thorough examination of the changes in expansive soil's geotechnical properties by conducting a series of laboratory studies and studying the hydration reaction process of the soil brought on by the use of bagasse ash. The laboratory studies include the soil strength test, compaction properties, swelling characteristics, soil stiffness anisotropy, and finally X-ray diffraction and scanning electron microscope tests to look into the material's compositions and microstructures, respectively.

## 2 Material and Methods

### 2.1 Material

#### 2.1.1 Expansive Soil

The soil used in this study is a mixture of 1:3 bentonite and natural soil. The natural soil was obtained from a forest park hill in Dalian City, Liaoning Province, China. Bentonite is a type of silicate clay with properties of absorption, swelling, and cation exchange. The particle analysis test can quantitatively reflect the different particle sizes in soil and provide a basis for analyzing the gradation of soil. The Atterberg limits of the soil were about 50.1% for the liquid limit and 18.9% for the plastic limit, which led to a plasticity index of 31.2. The particle size result is shown in Fig. 1. The wet sieve analysis was used to study soil particle sizes ranging from 0.075 mm to 1 mm, while the hydrometer analysis test was used for particles less than 0.075 mm. The one-dimensional free swell (swelling ratio) of the soil is

21.6%. Therefore, this soil can be judged according to plasticity as a weak expansive soil. Using the ASTM D698 standard [17], the optimum water content (OMC) and maximum dry density (MDD) are 23.28% and 1.61 g/cm<sup>3</sup> (100.51 lb/ft<sup>3</sup>), respectively.

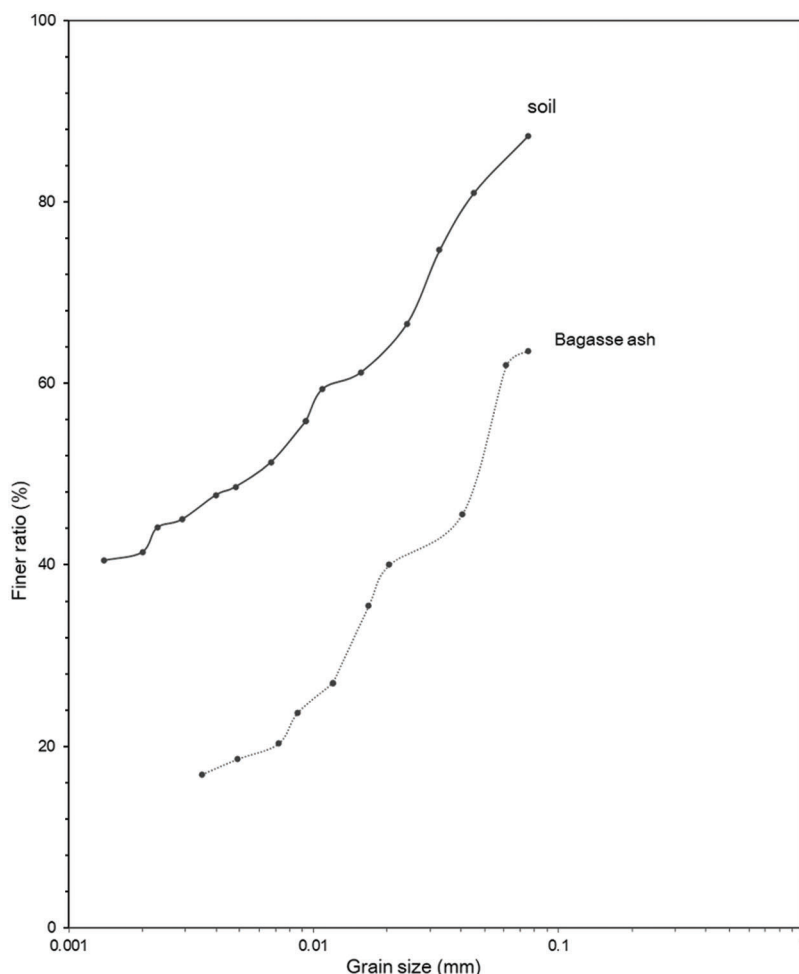


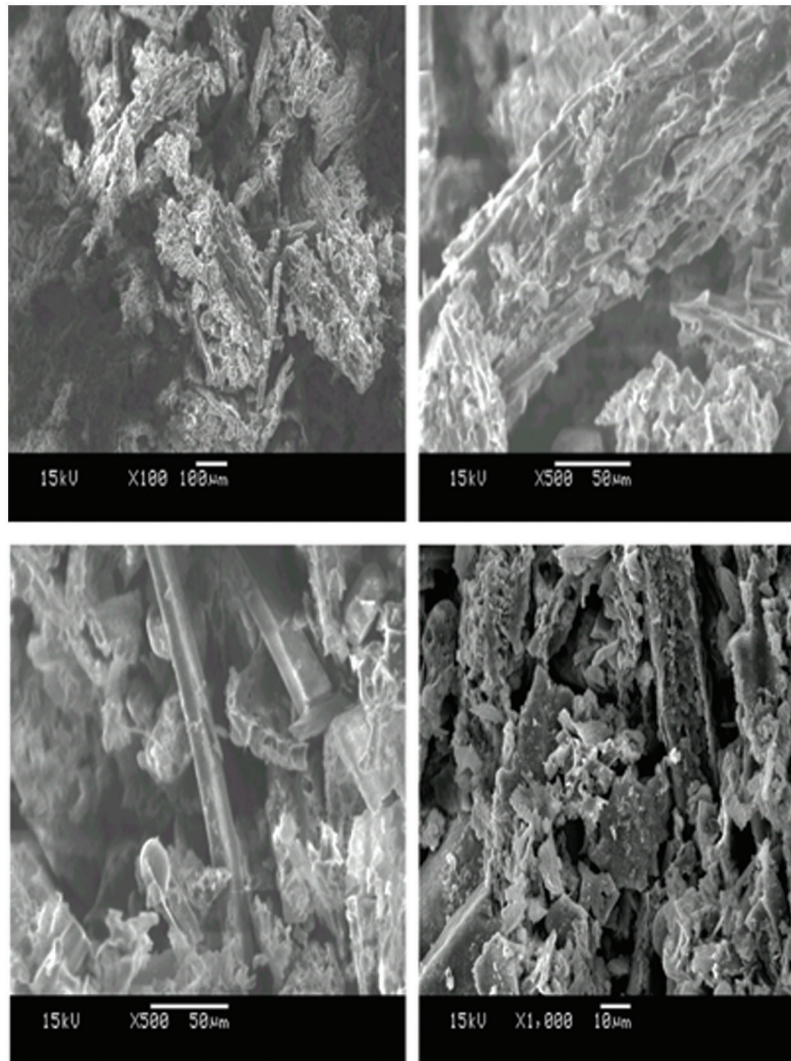
**Figure 1:** The soil and bagasse ash's particle size distribution

### 2.1.2 Bagasse Ash

Bagasse ash contains a significant amount of calcium, silica, and aluminum oxides. Due to its high reactive activity, it is considered to be a promising pozzolanic material that might be used in expansive soil stabilization. Bagasse ash was purchased from a commercial company in Nanning, Guangxi Province, China, for this investigation. The chemical composition of bagasse ash as determined by X-ray fluorescence (XRF) analysis is shown in Table 1. With 59.69% SiO<sub>2</sub>, 10.3% CaO, and 8.56% MgO, it has a good pozzolanic material. It has a specific gravity of 1.69 g/cm<sup>3</sup>, which is lower than soil and cement [18] when measured according to the ASTM D854-14 standard [19]. Wet sieve analysis and hydrometer analysis are used to determine the grain size distribution of bagasse ash, as shown in Fig. 1. Bagasse ash was subjected to a scanning electron microscope (SEM) test. The SEM images are shown in Fig. 2.

**Table 1:** The chemical composition of bagasse ash and cement

Bagasse ash											
Item	SiO <sub>2</sub>	CaO	Fe <sub>2</sub> O <sub>3</sub>	MgO	K <sub>2</sub> O	MnO	P <sub>2</sub> O <sub>5</sub>	TiO <sub>2</sub>	Al <sub>2</sub> O <sub>3</sub>	ZnO	Other
%	59.7	10.3	8.64	8.56	5.4	2.3	2	1.2	0.76	0.6	0.44
Cement											
%	23.13	62.6	3.31	0	1.34	0.076	0.08	0.48	4.8	0.06	0.394

**Figure 2:** SEM images of Bagasse ash sample

Bagasse ash samples were found to consist of grains of various sizes and shapes, as seen in SEM pictures. There are a bunch of stick-shaped particles, and some of them connect to form a thick cylinder-shaped particle. A single stick-shaped particle can be over 300 μm long and have a diameter of 7 to 8 μm. In the SEM image, there are also several small micro-solid particles. The XRD data for

bagasse ash is shown in Fig. 3. Silicate (Q) and cristobalite are the two most common minerals found in bagasse ash.

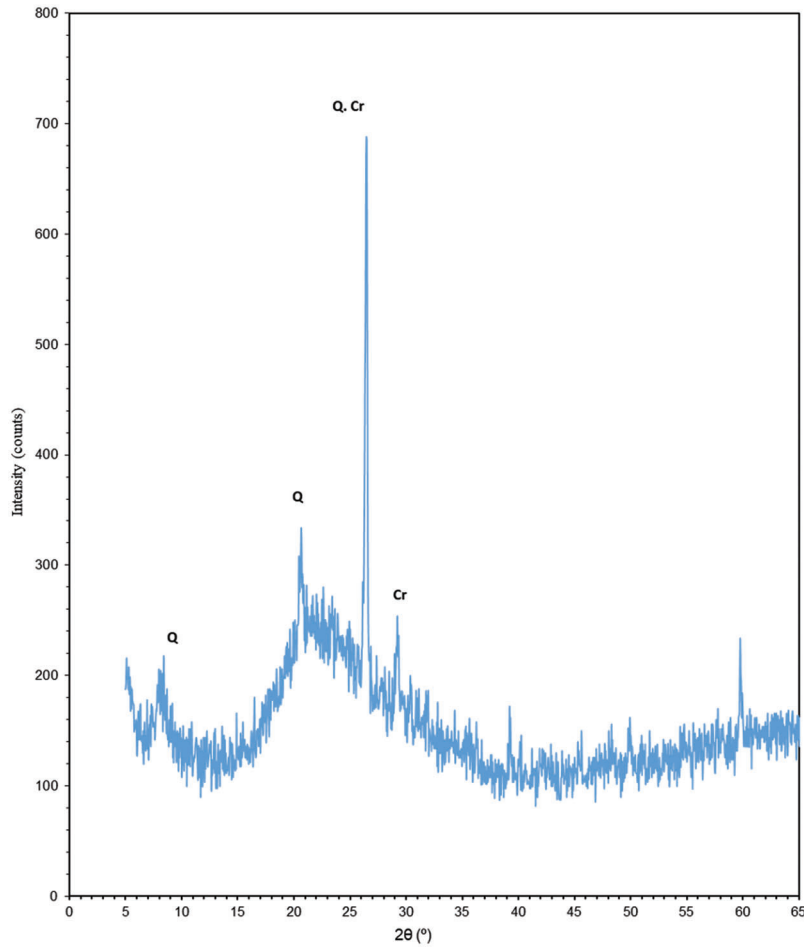


**Figure 3:** XRD results for bagasse ash (Q: quartz, Cr: cristobalite)

### 2.1.3 Ordinary Portland Cement (OPC)

In this study, ordinary Portland cement was employed. The cement was procured from a cement mill in the Chinese City of Dalian. Table 1 summarizes the chemical composition of cement, as determined by XRF testing. When compared to bagasse ash, cement has a larger percentage of CaO but a lower amount of SiO<sub>2</sub>. Dry cement powder was also subjected to SEM testing. Fig. 4 shows images of cement taken using a scanning electron microscope. The majority of cement particles are less than 10 μm. The OPC used has a specific gravity of 3.1 g/cm<sup>3</sup> (193.5 lb/ft<sup>3</sup>).

### 2.1.4 Mix Proportion

The ratio of bagasse ash used to replace cement in treated soil was set at 0%, 10%, 20%, 30%, 40%, 60%, and 70% of the total dry mass of additives. The combined additives made up 5% of the dry mass of the soil. The cement-bagasse ash ratio by wet soil volume employed in the testing program is shown in Table 2. Based on the soil volume at OMC, the wet soil volume is determined.



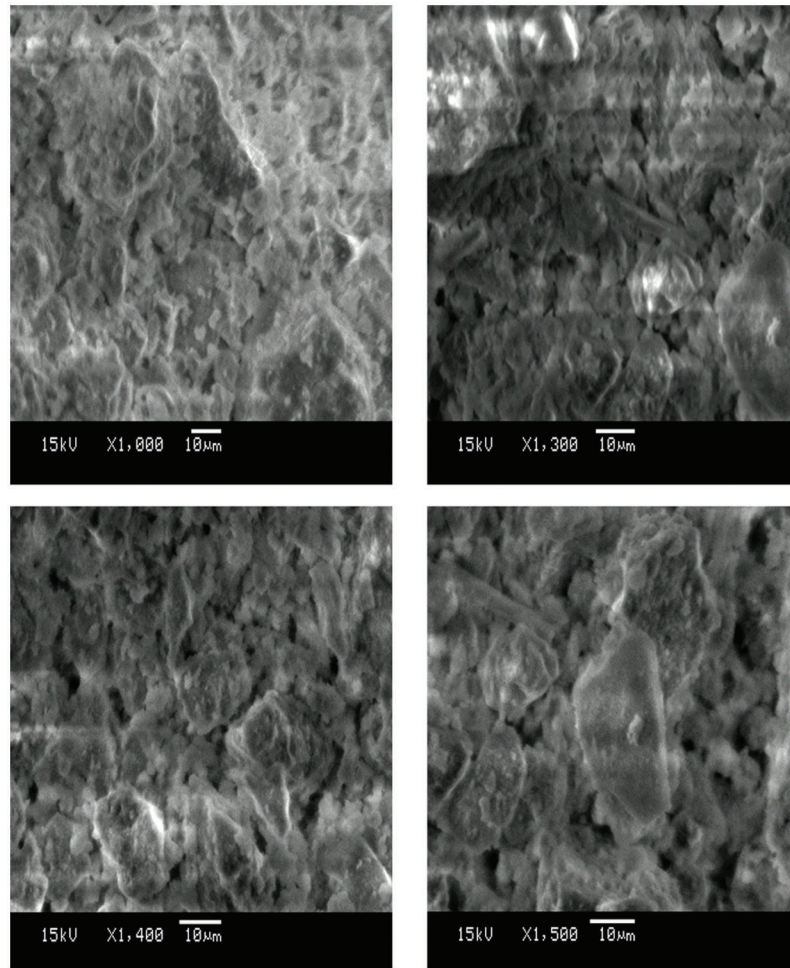


**Figure 4:** SEM image of dry cement powder

**Table 2:** The mixture proportion for specimens in the testing program

Symbol	The cement-Bagasse ash ratio (C:BA)	C ( $\text{kg/m}^3$ )/(lb/ft <sup>3</sup> )	BA ( $\text{kg/m}^3$ )/(lb/ft <sup>3</sup> )
CBA0	100:0	120(7.49)	0(0)
CBA10	90:10	108(6.74)	12(423.8)
CBA20	80:20	96(5.99)	24(847.6)
CBA30	70:30	84(5.24)	36(1271.3)
CBA40	60:40	72(4.49)	48(1695.1)
CBA60	40:60	48(3.00)	72(2542.7)
CBA70	30:70	36(2.25)	84(2966.4)

## 2.2 Methods

The series of lab tests carried out for this study are the compaction test, swelling index test, strength test, stiffness anisotropy test, X-ray diffraction test (XRD), and scanning electron microscope (SEM) tests.

The compaction test is conducted according to the ASTM D698 standard [17]. 42 test samples with varying dosages of cement and bagasse ash alongside the untreated soil were subjected to proctor compaction tests to determine the maximum dry density (MDD) and optimal water content (OMC).

The swelling index test is conducted in accordance with the ASTM D4546 standard [20]. A free swelling test was performed on 16 test samples of 20 mm in height and 61.8 mm in diameter (see Fig. 5A), which were classified into eight groups depending on the percentage of cement and bagasse ash present in the treated and untreated soil.

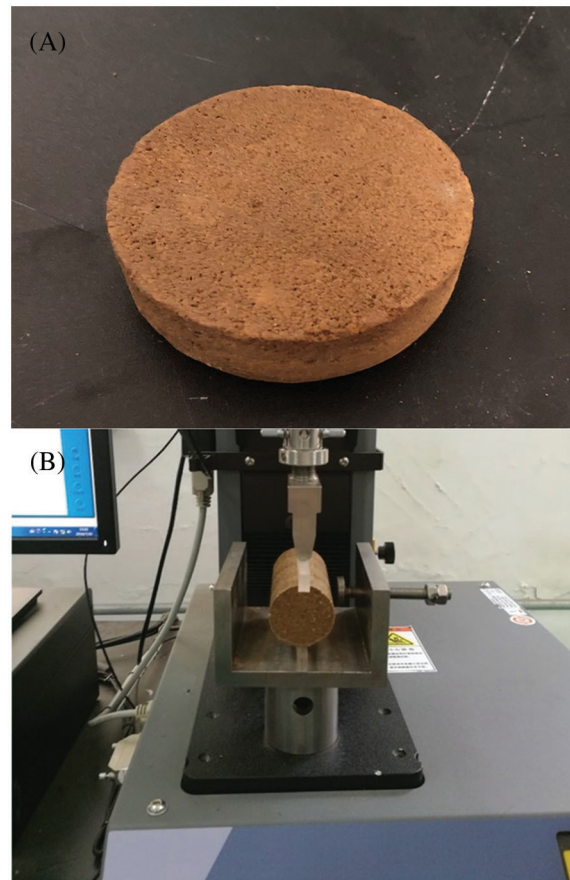


**Figure 5:** The shape of different samples used for the experiments

For the strength test, 45 test samples with a diameter of 39.1 mm and a height of 80 mm (see Fig. 5B), were formed, sealed, and cured in a laboratory environment at a constant humidity of 90% and a temperature of 25°C. The samples were then divided into three main groups based on the curing times (7, 14, and 28 days), and each group contained seven samples of soil treated with varying amounts of cement and bagasse ash (two samples were made for each percentage), in addition to the samples of plain soil, which were used for the unconfined compression (UCS) test. The same procedure of sample preparation was used for Brazil split tensile test. The test was carried out using the modified Akin et al. [21] method, while the unconfined compression test was carried out in line with ASTM D2166/ASTM D2166M-16.20 standards [22]. CBR tests were conducted based on the ASTM D1883 standard [23], and the eight samples used were soaked in the water for 96 h under a constant temperature of 25°C.



For the stiffness anisotropy, bender element (BE) tests were conducted according to a system designed by Kang et al. [24]. The BE used in this study was made from piezo ceramic plates (Piezo Systems, Inc., Cambridge, USA) with dimensions of 12.7 mm in length, 8.0 mm in width, and 0.6 mm in thickness.

For the XRD test, eight samples used in this test were all dried in an oven and ground into powder. The samples are sealed and maintained at a consistent humidity and temperature. For the plain soil next to the treated soil, the XRD was cured out. CuK $\alpha$  radiation was used for the XRD analysis on the Empyrean XRD equipment, with a 5° to 65° scanning angle.

For the SEM test, the experiment was carried out with methods that are frequently found in the literature. Samples of untreated soil and soil treated with various replacement ratios of cement and bagasse ash were collected after the 28-day curing group finished the UCS test. A portion of the examined samples was cut into small cubes, which were then completely cooled in liquid nitrogen and dried for approximately three hours in a vacuum freeze drier. The surface was cleaned with nitrogen, then gold was sprayed on, and the sample was then fastened to the cap with conductive adhesive tape before scanning.

### 3 Results and Discussion

#### 3.1 One-Dimension Free Swelling Test

The one-dimensional free swelling test on cement and bagasse ash with various replacement ratios also revealed 0% swelling, indicating a much better impact on swelling control. Previous studies have shown that soil specimens treated with cement alone have minimal expansion.

#### 3.2 MDD and OMC

Fig. 6 depicts the conventional compaction test results, while Table 3 lists MDD and OMC statistics. In comparison to natural soil, MDD has decreased. MDD drops at first and subsequently increases when bagasse ash content rises. The MDD of CBA20 is the lowest. The cation exchange between treated soil particles, which leads to aggregation and agglomeration [18], can explain this. In addition to the low specific gravity of bagasse ash, the structural change of the soil can be attributed to the drop in MDD.

OMC is clearly affected by the addition of cement and bagasse ash. In comparison to natural soil, OMC increased for all percentages of cement and bagasse ash, as shown in Fig. 6. This could be due to the pozzolanic reaction of silica and alumina in soil with calcium in cement, forming calcium silicate hydrate and calcium aluminate hydrate, which are the cementing agents and necessitate the use of more water [25].

#### 3.3 Unconfined Compressive Strength

Fig. 7 shows the UCS testing results for all specimens at various curing ages. At various curing times, UCS indicates an almost minimal change for CBA70. UCS increases for CBA60 and CBA40 at varied curing times, then reduces slightly after 7 days. UCS increases almost linearly with curing time for CBA0, CBA10, CBA20, and CBA30.

For tested samples, the maximum UCS value at various curing periods can be derived. At the age of 7 days of curing, the highest UCS for CBA10 was 451 kPa, 1017 kPa for CBA20 at 14 days of curing, and 2421 kPa for CBA0 at 28 days of curing. In general, the addition of cement and bagasse ash to the soil increased the strength of the soil significantly when compared to the test results of natural soil samples (180 kPa/26.1 psi). At 7, 14, and 28 days, the compressive strength of cement-treated expansive soil increases with curing time. The pozzolanic gel material created by the cement's hydration reaction improves the joint strength of the soil particles, and the amount of pozzolanic gel material grows and hardens as the curing time goes on, resulting in a significant improvement in the compressive strength of the treated soil. Brittle failure is the failure mode of cement-treated soil samples.

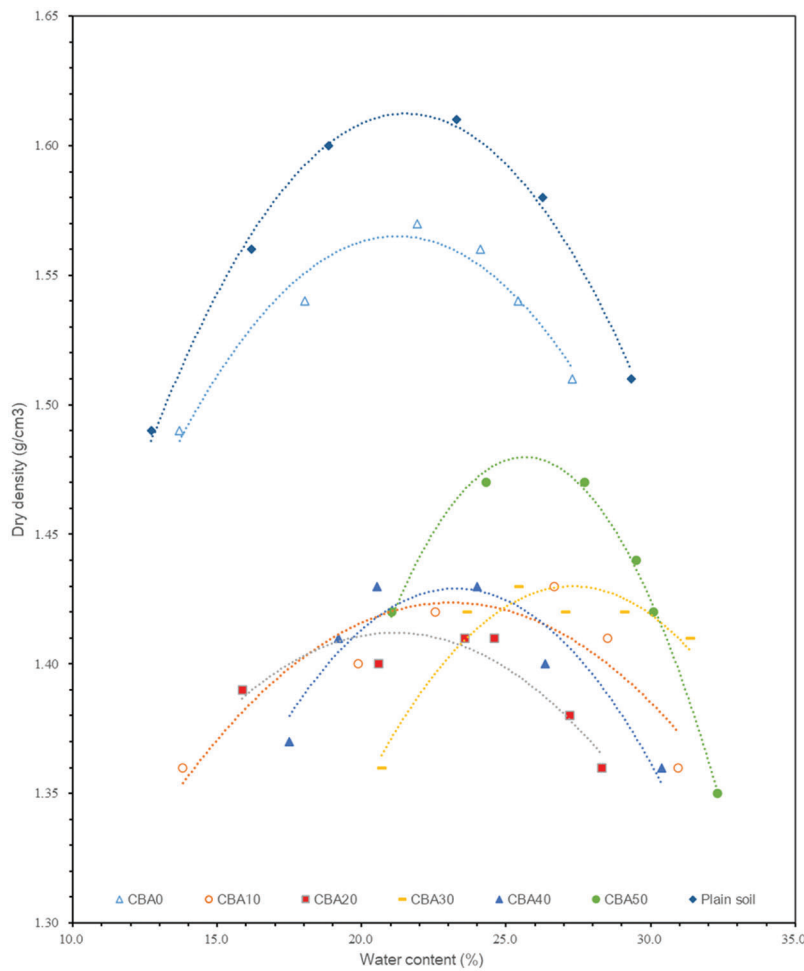


**Figure 6:** Compaction test results of treated soil and plain soil

**Table 3:** OMC and MDD for tested specimens

	Plain soil	CBA0	CBA10	CBA20	CBA30	CBA40	CBA50
OMC (%)	23.28	21.0	22.5	22.2	26.4	24	25.8
MDD (g/cm <sup>3</sup> )	1.61	1.57	1.43	1.41	1.44	1.43	1.47

Fig. 8 depicts the UCS vs. bagasse ash replacement ratio. The 20% replacement ratio yields the largest UCS at both 14 and 28 days, as seen in the graph. This is likely related to the fact that a 20% replacement ratio is required to produce  $\text{SiO}_2$  for the formation of hydration gel with the calcium provided by cement hydration. The partial replacement of cement with bagasse ash did not significantly alter the early strength of treated soil after 7 days of curing time. At 14 days of curing time, UCS increases significantly with a replacement ratio of less than 20% compared to natural expansive soil. After 28 days of curing, soils treated with 10%, 20%, and 30% bagasse ash replacement ratios had reasonably high UCS, while cement treated alone had a somewhat lower UCS. The 20% replacement ratio produces the greatest UCS value of all the replacement ratios. These findings are consistent with those of Ganesan et al. [26], who

determined that a cement replacement ratio of 20% is the best. This suggests that bagasse ash can be used to partially replace cement-treated soil on a temporary construction site or in conditions where a high UCS is not required, such as a country road. Thus, the construction costs will be reduced as a result of this.

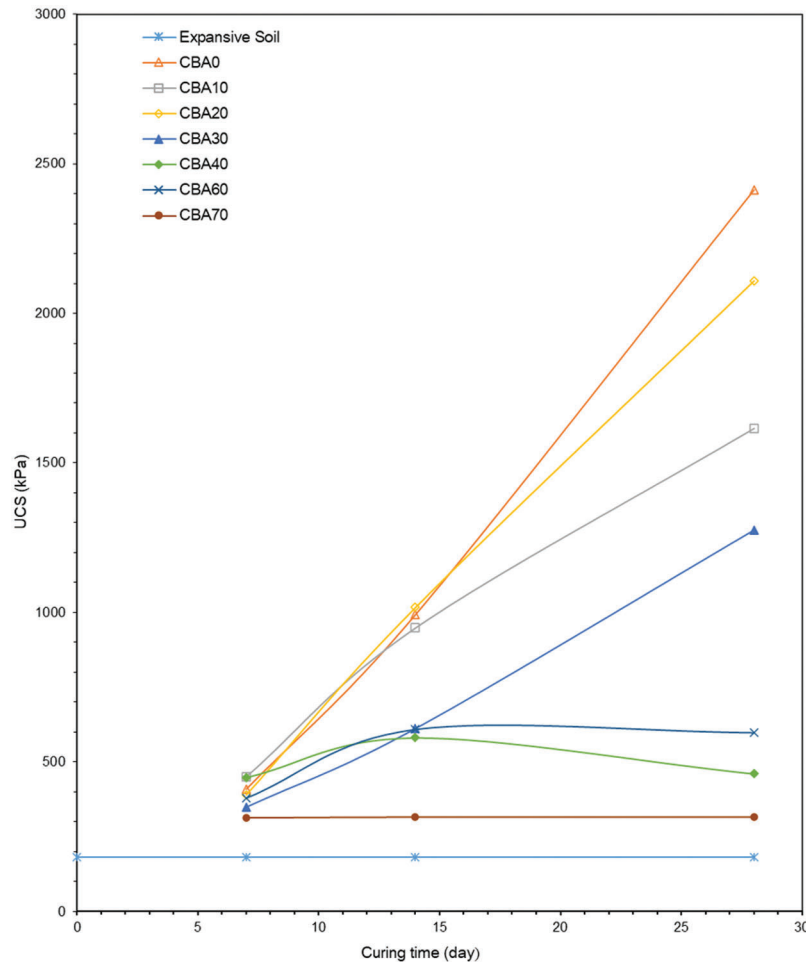


**Figure 7:** UCS test data for treated soils with curing time

### 3.4 CBR Test

The CBR test is a penetration test used to determine the strength of the subgrade of roads and pavements. It is used to assess the strength of soils that have been treated with bagasse ash and cement. The results of the CBR tests on various treated soils are given in Fig. 9. The CBR values often increase with the addition of cement and bagasse ash, as shown by the results. It can also be shown that when a small amount of bagasse ash is added to cement (CBA10, CBA20), the CBR values increase at first, and then steadily decline when more bagasse ash is added. The increase is likely due to the necessary amount of  $\text{Ca}^{2+}$  required for the synthesis of calcium silicate hydrate (CSH) and calcium aluminate hydrate (CAH), both of which are essential variables in boosting strength. The bagasse ash dissolves quickly in water and releases a substantial amount of  $\text{Ca}^{2+}$ , which is more than the amount released by cement alone, because cement takes time to release all of the  $\text{Ca}^{2+}$ . The drop in CBR value could be owing to the addition of more bagasse ash to the soil; at this point,  $\text{SiO}_2$  is insufficient to generate more hydrating cementation products.

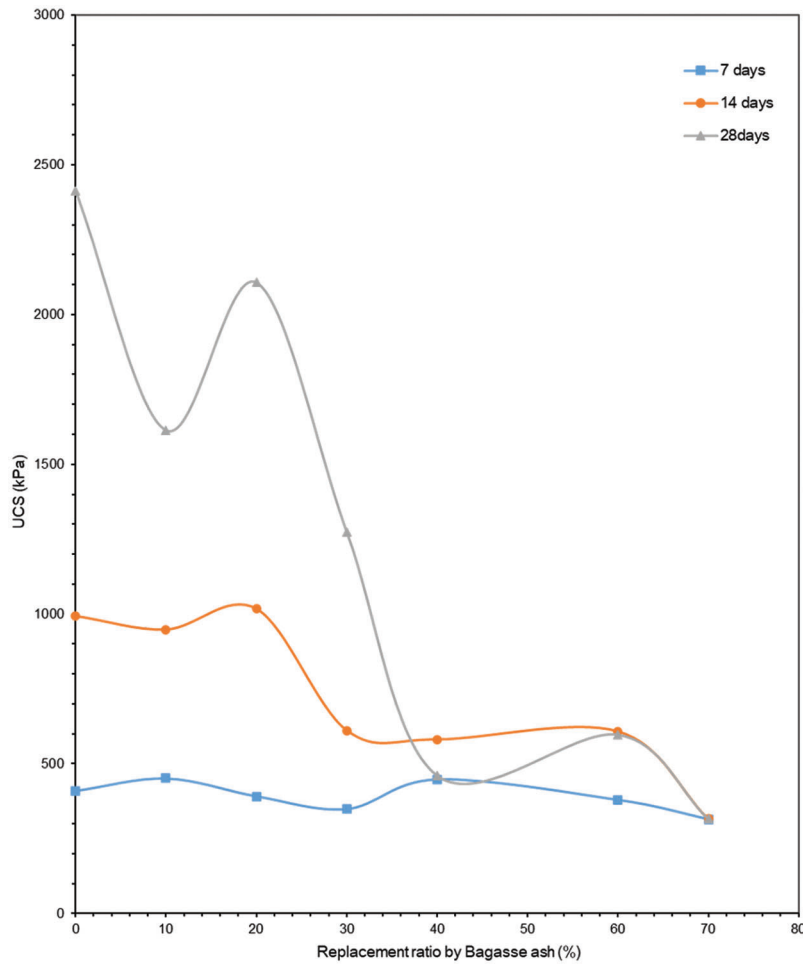


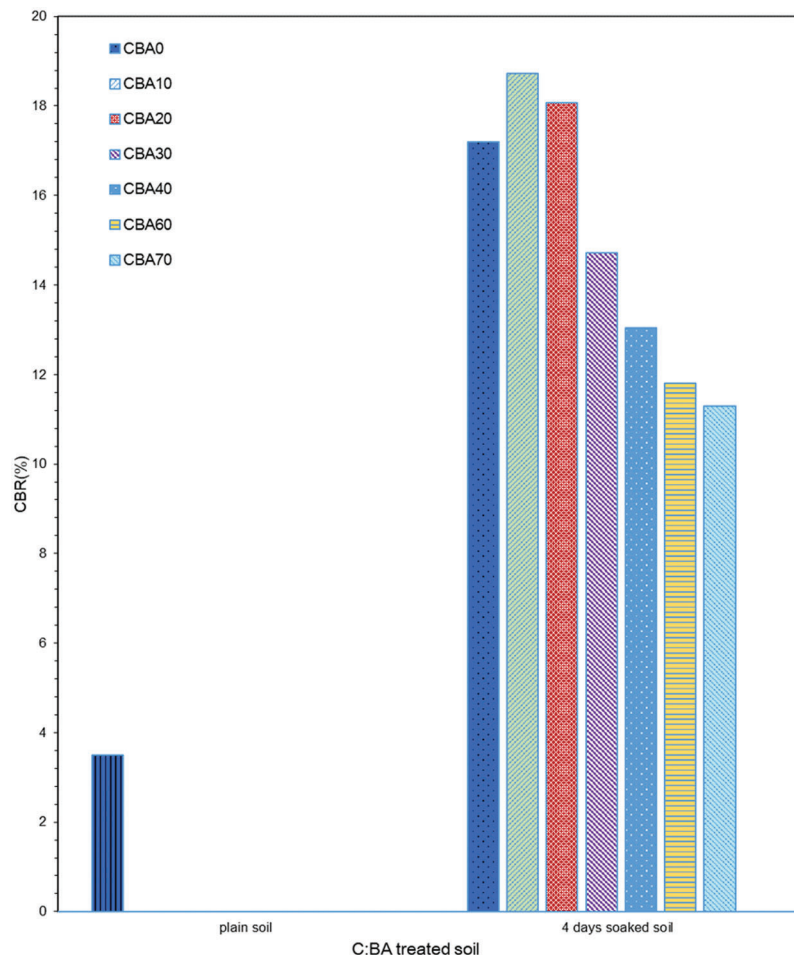
**Figure 8:** UCS test data for treated soils with replacement ratio

### 3.5 Indirect Tensile Strength Test

Tensile strength is important for treated soils because it regulates fracture formation in the soil. Thus, a series of Brazil split tensile tests were employed to evaluate the indirect tensile strength of treated specimens. Figs. 10 and 11 depict the tensile stress and displacement data for 7 and 28 days, respectively. The expansive soil's tensile stress vs. displacement curve is a strain softening type of failure. However, the treated soil's curve gradually shifted from strain-softening to brittle. The equation for calculating indirect tensile strength is:

$$T = \frac{2P}{\pi ld} \quad (1)$$

where  $T$  is the indirect tensile strength,  $P$  refers to the maximum applied load,  $l$  ( $l = 80 \text{ mm}/3.15 \text{ inch}$ ) and  $d$  ( $d = 39.1 \text{ mm}/1.54 \text{ inch}$ ) represent the length and diameter of the specimen, respectively.



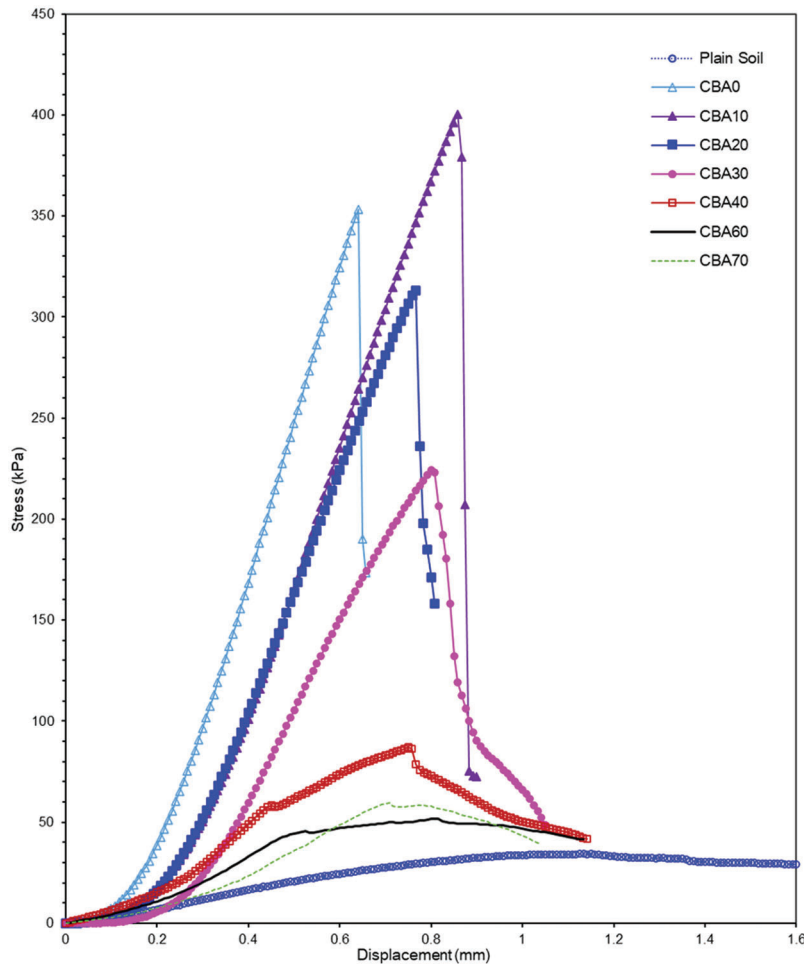
**Figure 9:** Soaked CBR test data for plain and treated soils

Fig. 12 summarizes the collected indirect tensile strength data. When comparing the treated and untreated soils, an increase in indirect tensile strength is often found. For each mixing ratio, the indirect tensile strength rose as the curing period increased. When only cement is supplied, the highest indirect tensile strength comes after 7 days of the curing period. However, as the curing time increased, the soil treated with 10% bagasse ash in place of cement had a higher indirect tensile strength than cement-treated soil. At 14 days of curing time, CBA0 has a higher indirect tensile strength than CBA20, CBA30, CBA40, CBA60, and CBA70. CBA20 has the highest indirect tensile strength after 28 days of curing. When measured during a 28-day curing period, 20% cement substitution with bagasse ash had the highest indirect tensile strength, which is 126% of the indirect tensile strength of samples treated just with cement. Cement-treated expansive soils are prone to cracking.

If the UCS values are higher than the design requirement, utilizing a fraction of bagasse ash instead of cement can improve the tensile strength of the treated soil while also saving cement, which is a better design alternative than using cement alone. As observed in CAB30, CAB40, CAB60, and CAB70, too much bagasse ash in place of cement results in decreased tensile strength. The higher the bagasse ash



concentration, the lower the tensile strength. This can be explained by the fact that too much bagasse ash inhibits the production of cementing elements, which are responsible for the treated expansive soil's tensile strength. The data on indirect tensile strength shows that there is an optimum replacement ratio for bagasse ash, which is also compatible with the UCS data observation.



**Figure 10:** Tensile test results after 7 days of curing

In Fig. 13, the gathered data of UCS and indirect tensile strength at various curing times is displayed. The data shows that the indirect tensile strength of CBA10, CBA20, and CAB30 increases with UCS, but not for CBA40, CBA60, or CBA70. The indirect tensile strength of cement-treated materials does not vary when the UCS increases. This means that the tensile strength of cement-treated expansive soils develops quickly within 7 days and then remains unchanged. The cement-bagasse ash treated expansive soils will gain more tensile strength with increasing curing time if the bagasse ash replacement ratio is no more than 30%.

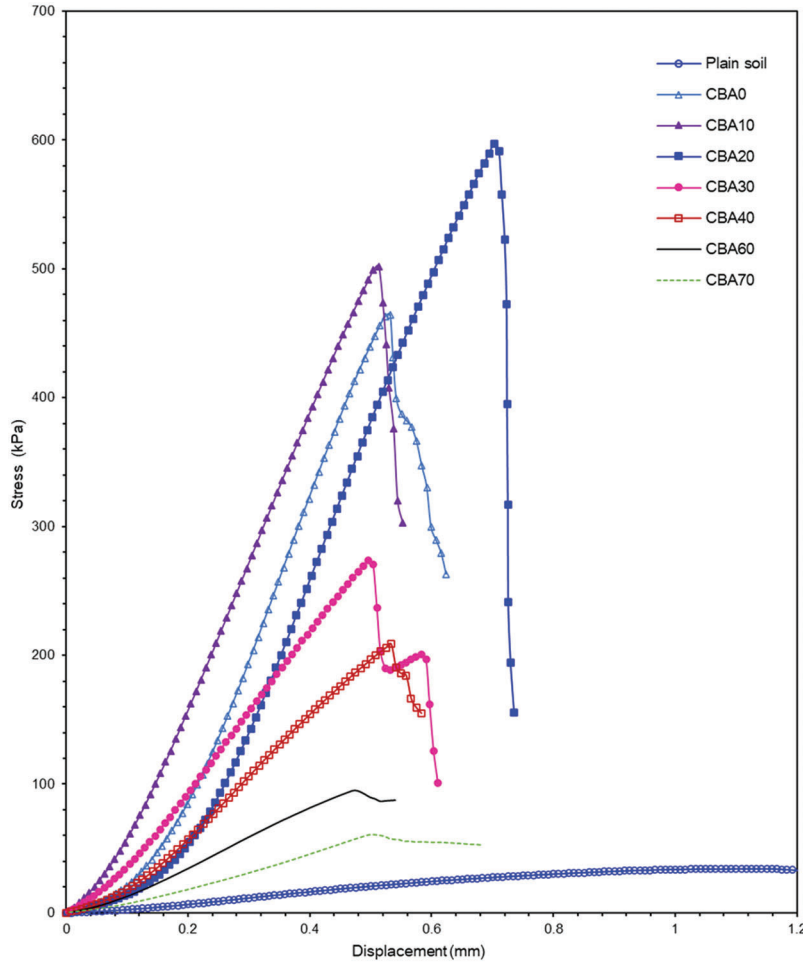


**Figure 11:** Tensile test results after 28 days of curing

### 3.6 Stiffness Anisotropy

Small strain stiffness of geo-materials is crucial in seismic zones for seismic design issues such as earthquakes, pile driving, traffic, and machine vibrations. However, only a few individuals have looked into the small strain stiffness of cement-expansive soil mixtures [27–29], not the bagasse ash-cement-expansive soil mixtures. Furthermore, the bagasse ash fiber and the compaction process may cause anisotropy in the treated soils, which has never been studied before. The initial shear modulus can be used to determine a soil's small strain stiffness ( $G_0$ ).  $G_0$  can be obtained by measuring shear wave velocity

$$G_0 = \rho \times V_s^2$$

where  $\rho$  is the mass density of the soil specimen. Nowadays, the BE test as a wave-based method has been successfully used in geotechnical engineering to estimate the small strain (less than  $10^{-3}\%$ ) shear modulus of soils [30]. Therefore, small strain stiffness and its anisotropy of treated soils are investigated through the BE testing method in this study.

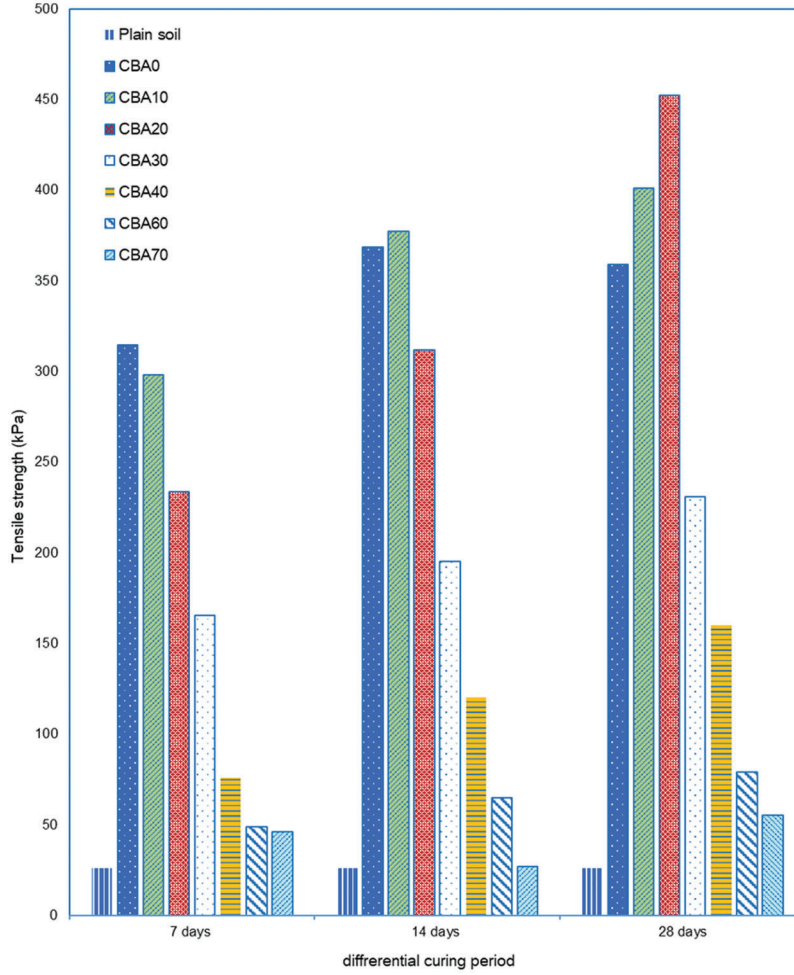


**Figure 12:** Tensile strength data of treated soils at different curing period

Fig. 14 depicts the bender element testing setup used in this investigation. BE experiments were carried out in three distinct directions to investigate the anisotropic features of the small-strain shear modulus, as shown schematically. In different directions, measured shear wave velocity is denoted as  $V_{s-ij}$ , where  $i$  indicates the direction of shear wave propagation and  $j$  indicates the direction of soil particle vibration, i.e.,  $V_{s-vh}$  indicates the shear wave is propagating vertically and soil particles are vibrating horizontally. With  $h \times d = 39.1 \text{ mm} \times 80 \text{ mm}$ . The specimen is prepared in the same way as for UCS.

The measured shear wave velocity values at different curing periods of 7, 14, and 28 days are shown in Fig. 15. From the results, at 7 days, the shear wave velocity  $V_{s-vh}$ ,  $V_{s-hh}$  and  $V_{s-hv}$  are not changing monotonically, in general,  $V_{s-vh} > V_{s-hh} > V_{s-hv}$ , with the replacement ratio of 70%, they tend to show the same value of 430 m/s,  $V_{s-hh}$ , and  $V_{s-hv}$  have a small difference since both are measured from the horizontal direction. The reason that  $V_{s-vh}$  is greater than  $V_{s-hh}$  and  $V_{s-hv}$  is probably because the bagasse ash fiber is parallel to the vertical plane due to compaction when making the specimen. The sample material is more continuous in this direction. When the replacement ratio reaches 70%, there are more bagasse ash fibers distributed both in the horizontal and vertical directions. Therefore, the three shear wave velocity values are the same.

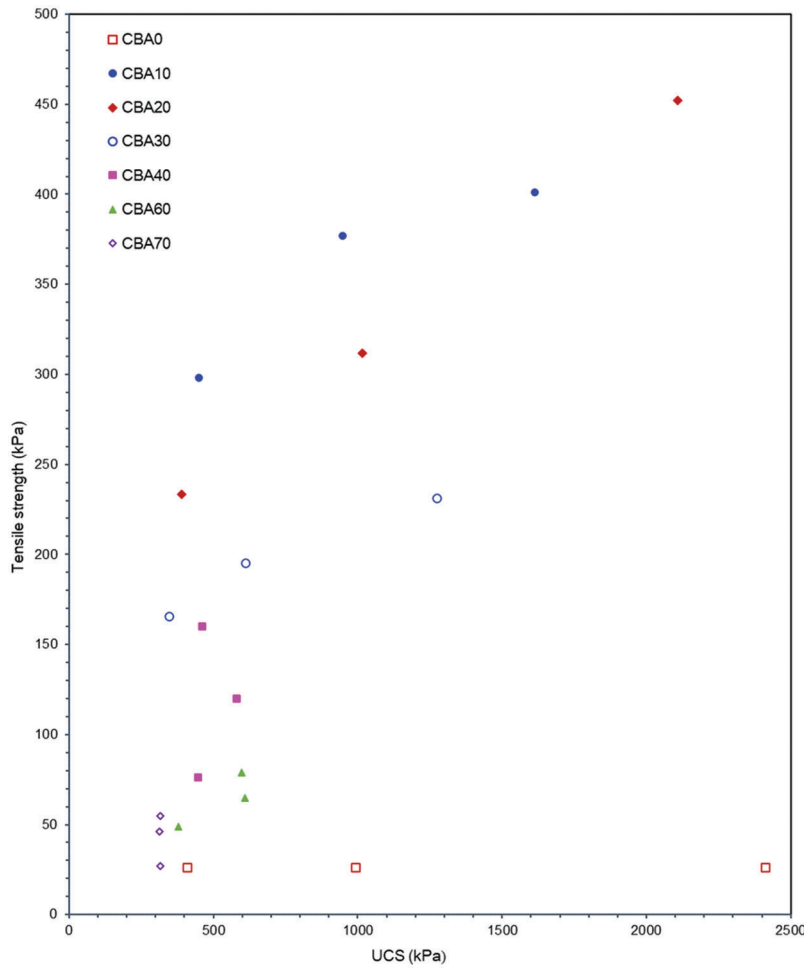


**Figure 13:** Tensile strength vs. UCS

On the whole, the shear wave velocity at 14 days of curing is slightly larger than that at 7 days. In general,  $V_{s-vh} > V_{s-hh} > V_{s-hv}$ , with the replacement ratio of 70%, they are getting to the same value of 460 m/s,  $V_{s-hh}$  and  $V_{s-hv}$  are also close to each other. These observations are similar to those of 7-day cured samples.

The shear wave velocity in three directions tends to be consistent across a 28-day curing period, decreasing first and then increasing with the increase in bagasse ash content, and then decreasing to a constant value of roughly 320 m/s, which is lower than the values at 7 and 14 days. The completion of hydration and solidification of cement and bagasse ash may result in all particles sticking tightly together, producing big particles and losing direction preference, resulting in consistency of shear wave velocity in three directions. Shear wave velocity decreases when the replacement ratio is less than 10% because cement hydration is primarily responsible for tying together soil particles. It increases when the replacement ratio rises because cement hydration and bagasse ash hydration are now jointly in charge of particle bonding. Finally, it decreases when cement content gradually decreases as well as the hydration cementation effect. The stiffness of treated expanding soils decreases in tandem. When the replacement ratio is less than 30%, shear wave velocity increases with curing time.

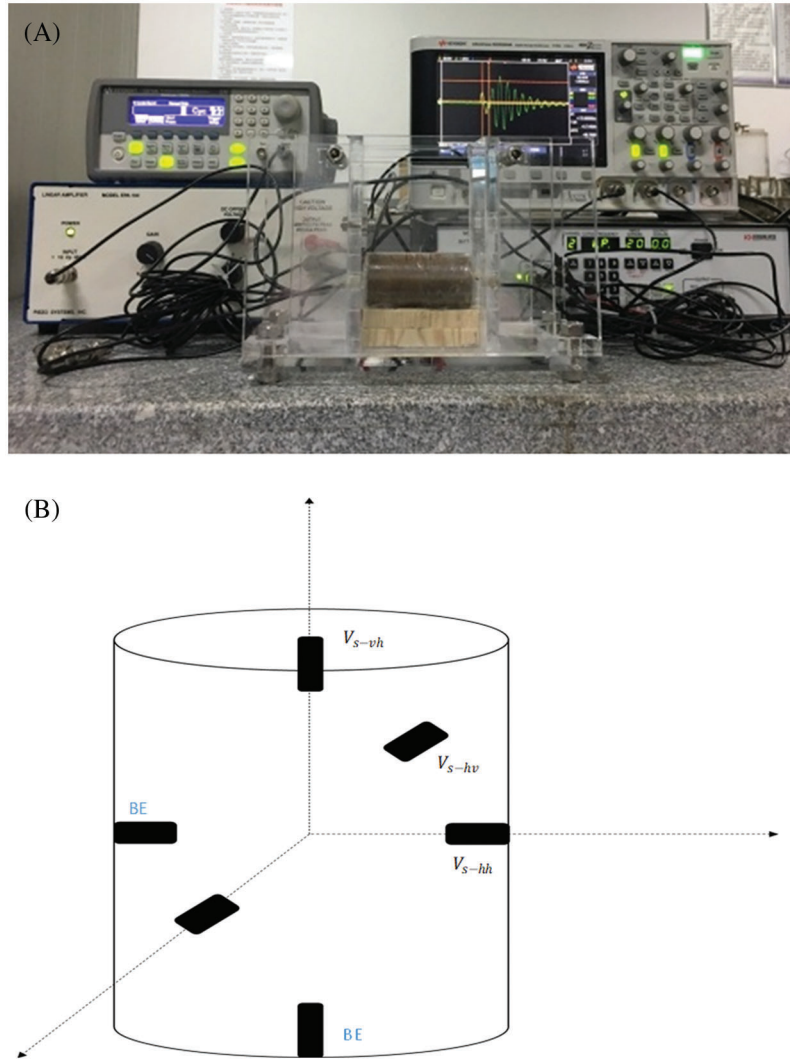


**Figure 14:** Bender element testing system: (A) photo; (B) schematic of testing directions

The anisotropic stiffness properties of treated soils were represented in the varied shear wave velocity measurements. In Fig. 16, the ratios measuring fabric-induced stiffness anisotropy, i.e.,  $G_{ivh}/G_{ihh}$ ,  $G_{ivh}/G_{ihv}$  and  $G_{ihh}/G_{ihv}$  ( $i=1, 2, 3$  indicating measures at 7, 14, and 28 days, respectively) are plotted. The specimens clearly display significant stiffness anisotropy during early curing times of 7 and 14 days, while reducing anisotropy at 28 days. The anisotropy ratio is highest after 7 days after the cure.  $G_{vh}/G_{hh}$  varies from 0.81% to 2.29%,  $G_{hv}/G_{vh}$  varies from 0.82% to 3.34%, and  $G_{hh}/G_{hv}$  varies from 0.80% to 1.57%, according to the testing results. Wang et al. [29] evaluated the small-strain shear-modulus anisotropy in soils, stating that  $G_{hh}/G_{hv}$  ( $G_{vh}/G_{hh}$ ) ranges from 1.0% to 2.60% (0.38% to 1.0%) and  $G_{hv}/G_{hh}$  ranges from 0.98% to 1.42%. The anisotropy ratios found here are significantly higher than those found by Wang et al. [29]. The small-strain stiffness anisotropy created is largely owing to the particle's fabric in the specimen and partly due to the compaction caused stress, because no load was applied to the specimens.



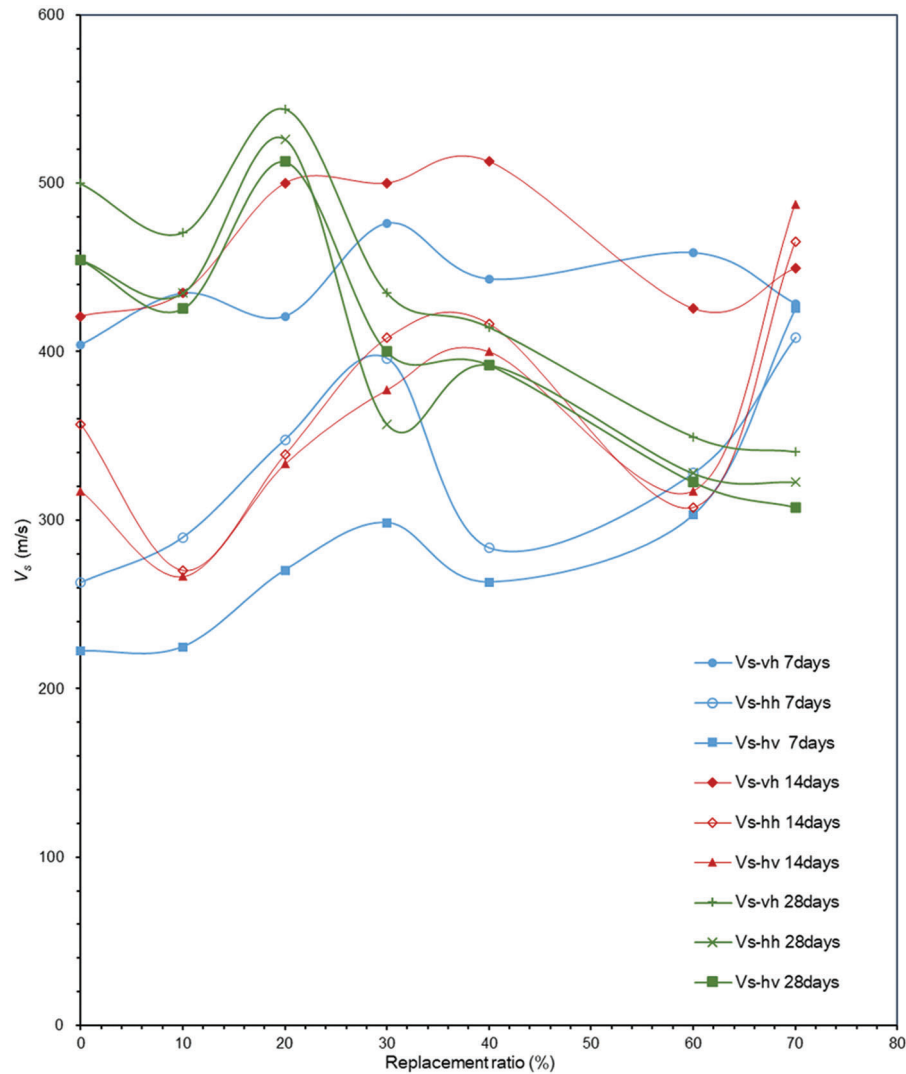


**Figure 15:** Shear wave velocity vs. replacement ratio after 7, 14, and 28 days of curing

### 3.7 XRD Test

After 28 days of curing, the XRD results for treated and untreated soil samples reveal that the soil is predominantly quartz with a very small amount of montmorillonite. When treated with cement and different amounts of bagasse ash, calcium silicate hydrate (CSH) gel and calcium hydroxide (CH) are the two essential components of the hydration products created by the pozzolanic reaction. As the curing time increases, calcium hydroxide may react with the silica and alumina in the soil to produce calcium silicate cementitious products and calcium met-aluminate products. The chemical reaction equations are as follows: (2) and (3). The main XRD pattern did not change much from Fig. 17, but new peaks of calcium silicate hydrate (CSH) are found at  $2\theta = 30^\circ\text{--}31^\circ$  and small calcium hydroxide (CH) peaks are formed at  $2\theta = 47.4^\circ$  and  $54^\circ$  with bagasse ash replacement ratios up to 20%, while the peaks of montmorillonite at  $2\theta = 28^\circ$  vanish or decrease in some specimens (i.e., CBA0, CBA10, CBA20, and CBA30). A cristobalite peak appears as the bagasse ash ratio rises (i.e., CBA30).

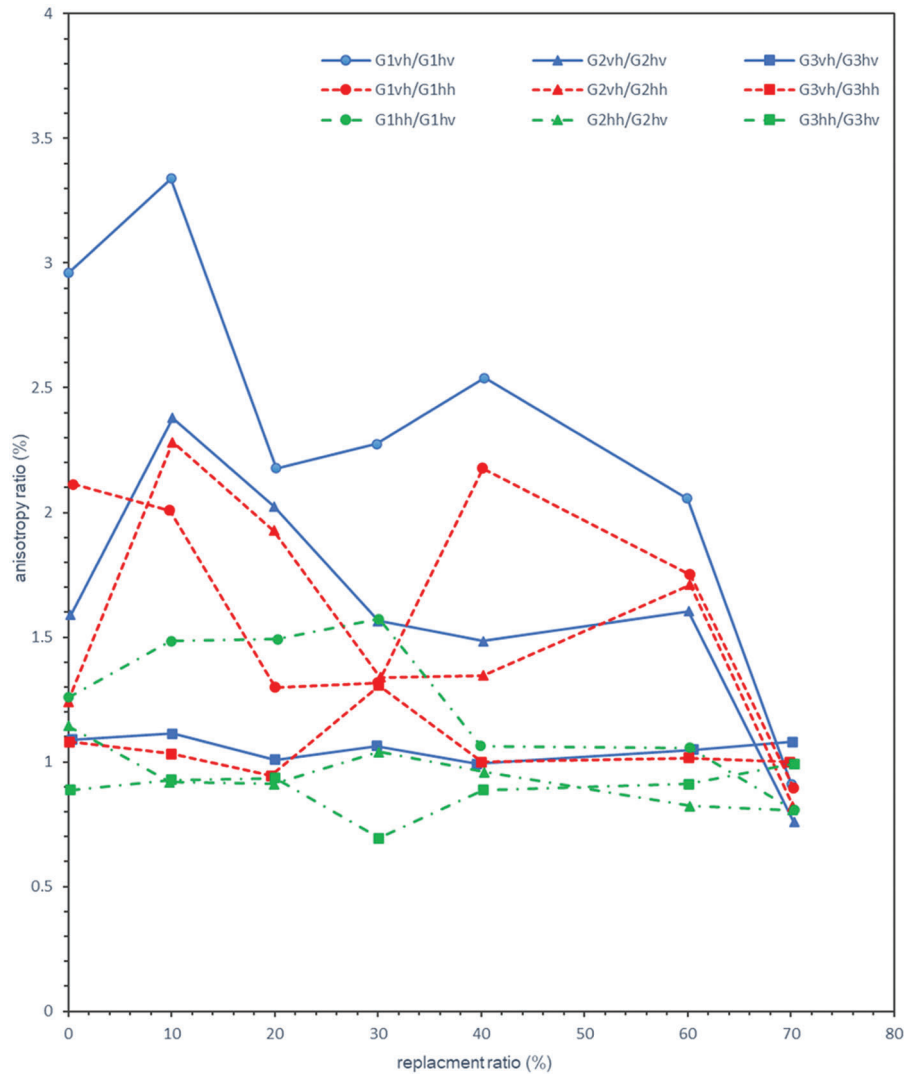
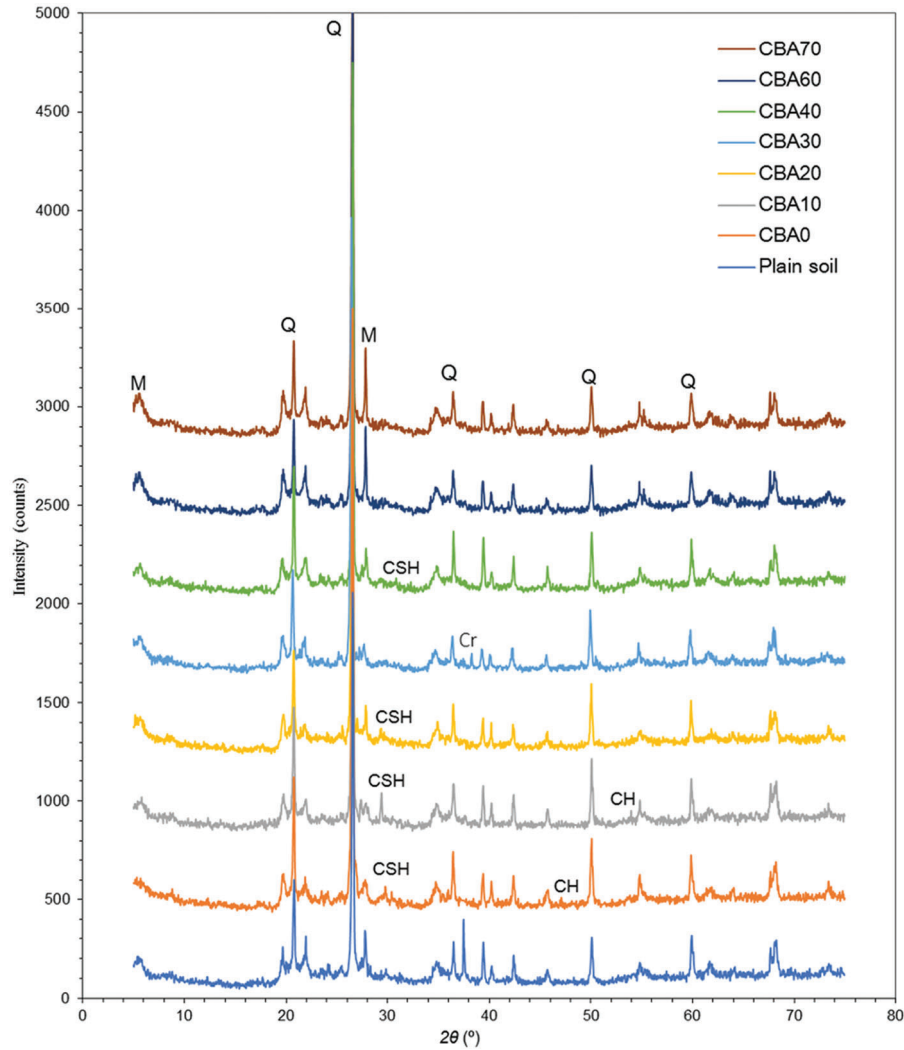


**Figure 16:** Anisotropic characteristics of treated expansive soils

### 3.8 SEM Test

The pore structure of the soil samples and the spaces between the soil particles may be seen in Fig. 18A. The loose, expansive soil has voids between the soil particles. In comparison to the treated soil, there are more evenly distributed tiny soil particles. After mixing with 5% cement, the CSH products formed by the cement hydration process join the soil particles, forming big aggregates, and the scattered tiny particles are no longer visible, with less porosity observed as seen in Fig. 18B. As the bagasse ash replacement ratio increases, soil particles become less dense as compared to those treated just with cement, and more bagasse ash fiber connections emerge between particles, as seen in Figs. 18F and 18G.

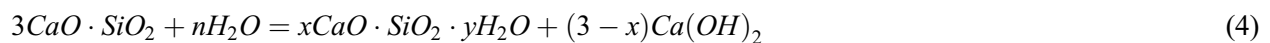
This is because, although there is a lot of  $\text{SiO}_2$  in bagasse ash, there is not enough  $\text{Ca}^{2+}$  to produce calcium silicate gel with less cement, and the cohesion between soil particles cannot join the small soil particles to form large aggregates. The 20% replacement soil specimens, on the other hand, have a tight structure with larger agglomerates forming.



**Figure 17:** XRD of untreated and treated expansive soils: Q: quartz, M: montmorillonite, Cr: cristobalite, CSH: calcium silicate hydrate, CH: calcium hydroxide

#### 4 Discussions

A complex hydration reaction process combined with a fiber strengthening effect can be characterized as the mechanism for partially replacing cement with bagasse ash to improve expansive soils. When cement is placed in the soil, it comes into contact with water and begins to disintegrate, releasing  $\text{Ca}^{2+}$  before hydrating to create calcium silicate hydrate. In the cement hydration process, there are three major pozzolanic reactions:





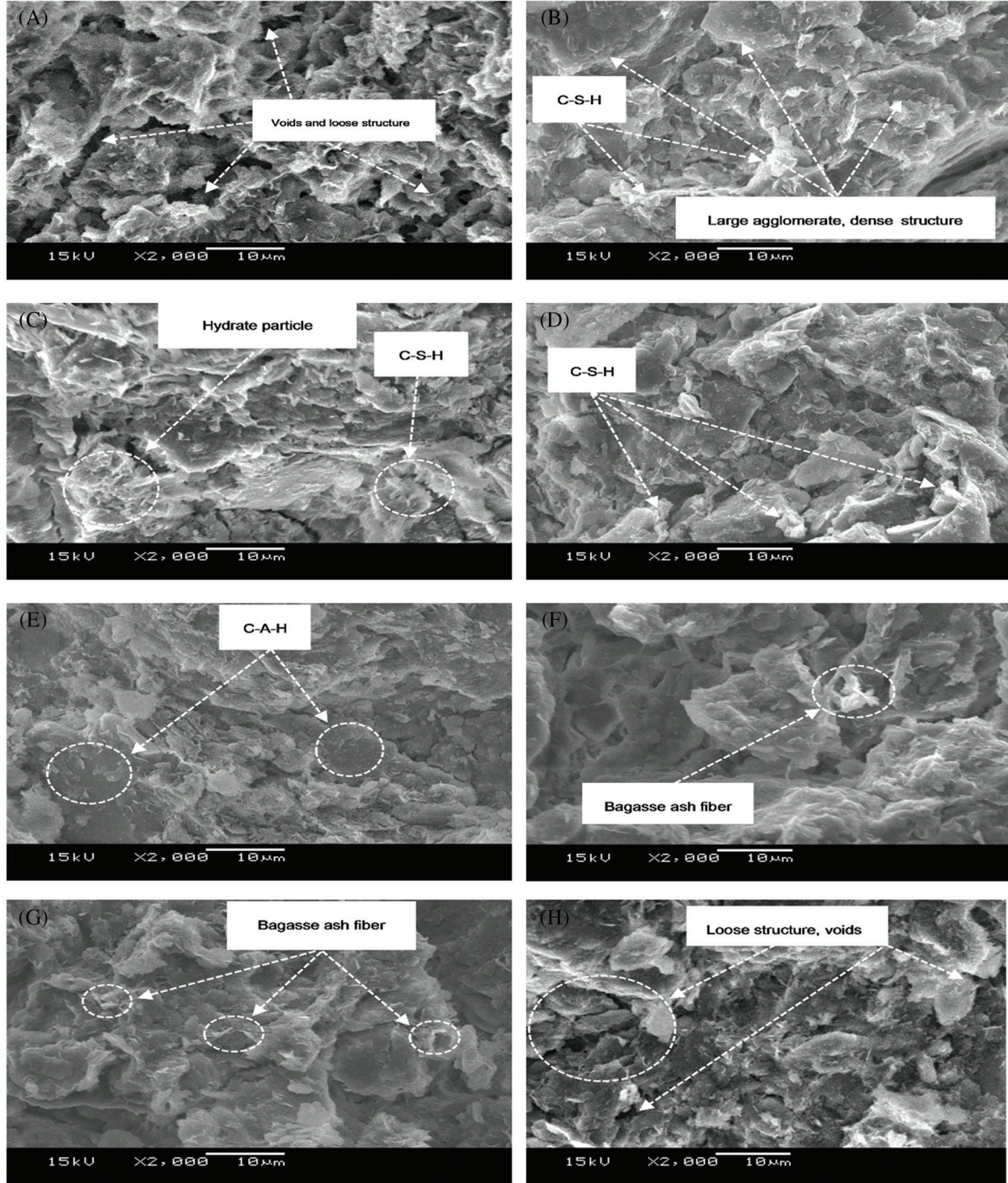
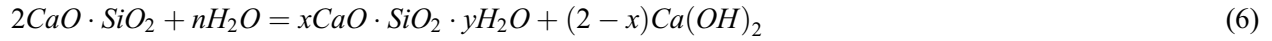


**Figure 18:** SEM testing results of untreated and treated samples: (A) plain soil; (B) CBA0; (C) CBA10; (D) CBA20; (E) CBA30; (F) CBA40; (G) CBA60; (H) CBA70. C: cement, BA: bagasse ash

The quantity of hydrate products produced is proportional to the amount of CaO and SiO<sub>2</sub> available. For the materials utilized in this study, bagasse ash contains around 10% CaO and 60% SiO<sub>2</sub>, while cement contains 62.6% CaO and 23.1% SiO<sub>2</sub>. When the replacement ratio is 20%, the ratio of CaO to SiO<sub>2</sub> approaches 1, which is the best ratio for a pozzolanic reaction to occur. This can explain why 20% is the optimum replacement ratio as observed in this study and also by Ganesan et al. [26]. Many studies have been conducted to determine whether adding fiber to soil can increase its tensile strength [31–33]. Bagasse ash fibers can be up to 30 µm long, allowing them to reinforce soil particles and resist tensile failure.

From the perspective of the interaction between macro and microproperties, the appropriate addition of cement and bagasse ash significantly improved the microstructure of the treated soil. The hydrate products bind the soil particles together and increase their macro-strength. The extra cement and bagasse ash filled the soil pores, which made the soil denser, as seen from the compaction results. The macro changes of UCS, CBR, and indirect tensile strength reflected the internal microstructure changes. Furthermore, the surface-encircling precipitate of the created hydrated cement significantly increases interfacial adhesion and boosts interface force and strength.

## 5 Conclusions

A series of laboratory tests were conducted using bagasse ash as a partial replacement for cement to stabilize the expansive soils. These test results would lead to the following conclusions:

In comparison to natural soil, OMC of treated soils increased for all cement and bagasse ash percentages, while MDD decreased as bagasse ash concentration increased. The optimum substitute ratio of 20% with increasing curing time corresponds to the maximum value of both unconfined compressive strength and tensile strength. Replacement ratios of 10% and 20% can result in CBR values that are comparable with the soil that has been treated with cement alone. The CBR of bagasse ash-replaced soil is lower than that of cemented-treated soils, but it is still higher than that of untreated soils. It is strongly recommended to use bagasse ash to replace cement to stabilize the expansive soils, which is a green method.

A helpful method to characterize the small strain stiffness and anisotropy of treated expansive soils is to measure the BE shear wave velocity. The fiber orientation created during specimen preparation, which is only present in the early phases, is what causes the anisotropy of the treated soil.

**Acknowledgement:** The authors are greatly appreciated. The bender element tests are conducted in the Laboratory of the Civil Engineering School of Hunan University with the help of Professor Xin Kang. The authors are very grateful for the help.

**Funding Statement:** This research is funded by the National Natural Science Foundation of China (Nos. 11672066, 12172085).

**Conflicts of Interest:** The authors declare that they have no conflicts of interest to report regarding the present study.

## References

1. Suksiripattanapong, C., Sakdinakorn, R., Tiyasangthong, S., Wonglakorn, N., Phetchuay, C. et al. (2022). Properties of soft Bangkok clay stabilized with cement and fly ash geopolymer for deep mixing application. *Case Studies in Construction Materials*, 16(4), e01081. DOI 10.1016/j.cscm.2022.e01081.
2. Khan, S. H. (2019). Use of gypsum and bagasse ash for stabilization of low plastic and high plastic clay. *Journal of Applied Research on Industrial Engineering*, 6(3), 251–267.
3. Nelson, J., Miller, D. (1992). *Treatment of expansive soils problem and practice in foundation and pavement*. New York: John Wiley and Sons.



4. Raja, P. S. K., Thyagaraj, T. (2021). Significance of compaction time delay on compaction and strength characteristics of sulfate resistant cement-treated expansive soil. *Journal of Rock Mechanics and Geotechnical Engineering*, 13(5), 1193–1202. DOI 10.1016/j.jrmge.2021.03.003.
5. Chenarboni, H. A., Lajevardi, S. H., MolaAbasi, H., Zeighami, E. (2021). The effect of zeolite and cement stabilization on the mechanical behavior of expansive soils. *Construction and Building Materials*, 272(1), 121630. DOI 10.1016/j.conbuildmat.2020.121630.
6. Zerihun, B., Yehualaw, M. D., Vo, D. H. (2022). Effect of agricultural crop wastes as partial replacement of cement in concrete production. *Advances in Civil Engineering*, 2022(4), 1–31. DOI 10.1155/2022/5648187.
7. Dang, L. C., Khabbaz, H., Ni, B. J. (2021). Improving engineering characteristics of expansive soils using industry waste as a sustainable application for reuse of bagasse ash. *Transportation Geotechnics*, 31(12), 100637. DOI 10.1016/j.trgeo.2021.100637.
8. Mollamahmutoglu, M., Avci, E. (2018). Engineering properties of slag-based superfine cement-stabilized clayey soil. *ACI Materials Journal*, 115(4), 541–548. DOI 10.14359/51701924.
9. Bahadori, H., Hasheminezhad, A., Taghizadeh, F. (2019). Experimental study on marl soil stabilization using natural pozzolans. *Journal of Materials in Civil Engineering*, 31(2), 04018363. DOI 10.1061/(ASCE)MT.1943-5533.0002577.
10. James, J., Pandian, P. K. (2018). Bagasse ash as an auxiliary additive to lime stabilization of an expansive soil: Strength and microstructural investigation. *Advances in Civil Engineering*, 2018(1), 1–16. DOI 10.1155/2018/9658639.
11. Zeidabadi, Z. A., Bakhtiari, S., Abbaslou, H., Ghanizadeh, A. R. (2018). Synthesis, characterization and evaluation of biochar from agricultural waste biomass for use in building materials. *Construction and Building Materials*, 181(11), 301–308. DOI 10.1016/j.conbuildmat.2018.05.271.
12. Khalil, M. J., Aslam, M., Ahmad, S. (2021). Utilization of sugarcane bagasse ash as cement replacement for the production of sustainable concrete—A review. *Construction and Building Materials*, 270(4), 121371. DOI 10.1016/j.conbuildmat.2020.121371.
13. Vital, A., Klotz, U., Marek, S., Jerzy, W. (2008). Silica aerogel; synthesis, properties and characterization. *Journal of Materials Processing Technology*, 199(1–3), 10–26. DOI 10.1016/j.jmatprotec.2007.10.060.
14. Li, Y., Chai, J., Wang, R., Zhang, X., Si, Z. (2022). Utilization of sugarcane bagasse ash (SCBA) in construction technology: A state-of-the-art review. *Journal of Building Engineering*, 56(5), 104774. DOI 10.1016/j.jobbe.2022.104774.
15. Li, Y., Wu, B., Wang, R. (2022). Critical review and gap analysis on the use of high-volume fly ash as a substitute constituent in concrete. *Construction and Building Materials*, 341(3), 127889. DOI 10.1016/j.conbuildmat.2022.127889.
16. Jha, P., Sachan, A. K., Singh, R. P. (2021). Agro-waste sugarcane bagasse ash (ScBA) as partial replacement of binder material in concrete. *Materials Today: Proceedings*, 44(2), 419–427. DOI 10.1016/j.matpr.2020.09.751.
17. ASTM D698-12e2 (2012). *Standard test methods for laboratory compaction characteristics of soil using standard effort (12 400 ft-lbf/ft<sup>3</sup> (600 kN-m/m<sup>3</sup>))*. West Conshohocken, PA: ASTM International.
18. Bowles, E. L. (1996). *Foundation analysis and design*. 5th edition. New York: The McGraw-Hill Companies.
19. ASTM D854-14 (2014). *Standard test methods for specific gravity of soil solids by water pycnometer*. West Conshohocken, PA: ASTM International.
20. ASTM D 4546-14e1 (2014). *Standard test methods for one-dimensional swell or collapse of soils*. West Conshohocken, PA: ASTM International.
21. Akin, I. D., Likos, W. J. (2017). Brazilian tensile strength testing of compacted clay. *Geotechnical Testing Journal*, 40(4), 608–617. DOI 10.1520/GTJ20160180.
22. ASTM D2166/D2166M-16 (2016). *Standard test method for unconfined compressive strength of cohesive soil*. West Conshohocken, PA: ASTM International.
23. ASTM D1883-16 (2016). *Standard test method for california bearing ratio (CBR) of laboratory-compacted soils*. West Conshohocken, PA: ASTM International.

24. Kang, X., Kang, G. C., Bate, B. (2014). Measurement of stiffness anisotropy in kaolinite using bender element tests in a floating wall consolidometer. *Geotechnical Testing Journal*, 37(5), 869–883. DOI 10.1520/GTJ20120205.
25. Ashango, A. A., Patra, N. R. (2016). Behavior of expansive soil treated with steel slag, rice husk ash, and lime. *Journal of Materials in Civil Engineering*, 28(7), 06016008. DOI 10.1061/(ASCE)MT.1943-5533.0001547.
26. Ganesan, K., Rajagopal, K., Thangavel, K. (2007). Evaluation of bagass ash as supplementary cementitious material. *Cement and Concrete Composites*, 29(6), 515–542. DOI 10.1016/j.cemconcomp.2007.03.001.
27. Bahador, M., Pak, A. (2012). Small-strain shear modulus of cement-admixed kaolinite. *Geotechnical and Geological Engineering*, 30(1), 163–171. DOI 10.1007/s10706-011-9458-1.
28. Chen, S. M., Wang, L. Z., Li, T. (2000). Experimental determination of dynamic properties of cement-treated soil v and earthquake behavior of composite foundation. *Journal-Zhejiang University Engineering Science*, 34(4), 398–403.
29. Wang, Y. H., Mok, C. M. (2008). Mechanisms of small-strain shear-modulus anisotropy in soils. *Journal of Geotechnical and Geoenvironmental Engineering*, 134(10), 1516–1530. DOI 10.1061/(ASCE)1090-0241(2008)134:10(1516).
30. Lee, J. S., Santamarina, J. C. (2005). Bender elements: Performance and signal interpretation. *Journal of Geotechnical and Geoenvironmental Engineering*, 131(9), 1063–1070. DOI 10.1061/(ASCE)1090-0241(2005)131:9(1063).
31. Consoli, N. C., de Moraes, R. R., Festugato, L. (2013). Parameters controlling tensile and compressive strength of fiber-reinforced cemented soil. *Journal of Materials in Civil Engineering*, 25(10), 1568–1573. DOI 10.1061/(ASCE)MT.1943-5533.0000555.
32. Festugato, L., da Silva, A. P., Diambra, A., Consoli, N. C., Ibraim, E. (2018). Modelling tensile/compressive strength ratio of fibre reinforced cemented soils. *Geotextiles and Geomembranes*, 46(2), 155–165. DOI 10.1016/j.geotexmem.2017.11.003.
33. He, S., Wang, X., Bai, H., Xu, Z., Ma, D. (2021). Effect of fiber dispersion, content and aspect ratio on tensile strength of PP fiber reinforced soil. *Journal of Materials Research and Technology*, 15, 1613–1621. DOI 10.1016/j.jmrt.2021.08.128.